AFRL-VA-WP-TP-2006-305

TRACKING CONTROL FOR AN OVERACTUATED HYPERSONIC AIR-BREATHING VEHICLE WITH STEADY STATE CONSTRAINTS (PREPRINT)

David O. Sigthorsson, Andrea Serrani, and Stephen Yurkovich
Michael A. Bolender and David B. Doman

DECEMBER 2005

Approved for public release; distribution is unlimited.

STINFO FINAL REPORT

AIR VEHICLES DIRECTORATE
AIR FORCE RESEARCH LABORATORY
AIR FORCE MATERIEL COMMAND
WRIGHT-PATTERSON AIR FORCE BASE, OH 45433-7542

NOTICE

PAO Case Number: AFRL/WS-06-0038, 04 Jan 2006.

THIS TECHNICAL REPORT IS APPROVED FOR PUBLICATION.

/s/

Michael A. Bolender
Aerospace Engineer
Control Design and Analysis Branch
Air Force Research Laboratory
Air Vehicles Directorate

/s /

Deborah S. Grismer
Chief
Control Design and Analysis Branch
Air Force Research Laboratory
Air Vehicles Directorate

/s/

Brian W. Van Vliet
Chief
Control Sciences Division
Air Force Research Laboratory
Air Vehicles Directorate

REPORT DOCUMENTATION PAGE	*Form Approved OMB No. 0704-0188*

1. REPORT DATE ***(DD-MM-YY)***	**2. REPORT TYPE**	**3. DATES COVERED** ***(From - To)***
December 2005	Conference Paper Preprint	12/01/2004 – 12/01/2005

4. TITLE AND SUBTITLE
TRACKING CONTROL FOR AN OVERACTUATED HYPERSONIC AIR-BREATHING VEHICLE WITH STEADY STATE CONSTRAINTS (PREPRINT)

5a. CONTRACT NUMBER F33615-01-C-3154
5b. GRANT NUMBER
5c. PROGRAM ELEMENT NUMBER 0601102

6. AUTHOR(S)
David O. Sigthorsson, Andrea Serrani, and Stephen Yurkovich (The Ohio State University)
Michael A. Bolender and David B. Doman (AFRL/VACA)

5d. PROJECT NUMBER A02D
5e. TASK NUMBER
5f. WORK UNIT NUMBER 0A

7. PERFORMING ORGANIZATION NAME(S) AND ADDRESS(ES)

The Ohio State University
Collaborative Center of Control Science
Dept. of Electrical and Computer Engineering
2015 Neil Avenue. Suite 205
Columbus, OH 43210

Control Design and Analysis Branch (AFRL/VACA)
Control Sciences Division, Air Vehicles Directorate
Air Force Research Laboratory
Air Force Materiel Command
Wright-Patterson AFB, OH 45433-7542

8. PERFORMING ORGANIZATION REPORT NUMBER

9. SPONSORING/MONITORING AGENCY NAME(S) AND ADDRESS(ES)
Air Vehicles Directorate
Air Force Research Laboratory
Air Force Materiel Command
Wright-Patterson Air Force Base, OH 45433-7542

10. SPONSORING/MONITORING AGENCY ACRONYM(S)
AFRL/VACA

11. SPONSORING/MONITORING AGENCY REPORT NUMBER(S)
AFRL-VA-WP-TP-2006-305

12. DISTRIBUTION/AVAILABILITY STATEMENT
Approved for public release; distribution is unlimited.

13. SUPPLEMENTARY NOTES
Conference paper preprint to be presented at the 2006 AIAA Guidance, Navigation, and Control Conference, 24 Aug 06, Keystone, CO. This report contains color.

14. ABSTRACT
This paper describes the design of a nonlinear control law for an air-breathing hypersonic vehicle. The model of interest includes flexibility effects and intricate couplings between the engine dynamics and flight dynamics. To overcome the analytical intractability of this model, a nominal control-oriented model is constructed for the purpose of feedback control design. Analysis performed on the nominal model reveals the presence of unstable zero dynamics with respect to the output to be controlled, namely altitude and velocity. By neglecting certain weaker couplings and resorting to dynamic extension at the input side, a simplified nominal model with full vector relative degree with respect to the regulated output is obtained. Standard dynamic inversion can then be applied to the simplified nominal model, and this results in approximate linearization of the nominal model. Finally, a robust outer loop control is designed using LQR with integral augmentation in a model reference scheme. Simulation results are provided to demonstrate that the approximate feedback linearization approach achieves excellent tracking performance on the truth model for two choices of the system output. Finally, a brief case study is presented to qualitatively demonstrate the robustness of the design to parameter variations.

15. SUBJECT TERMS Over-actuated Systems, Control Theory, Flight Control, Hypersonic Aircraft

16. SECURITY CLASSIFICATION OF:			**17. LIMITATION OF ABSTRACT:**	**18. NUMBER OF PAGES**	**19a. NAME OF RESPONSIBLE PERSON** (Monitor)
a. REPORT	**b. ABSTRACT**	**c. THIS PAGE**			Michael A. Bolender
Unclassified	Unclassified	Unclassified	SAR	24	**19b. TELEPHONE NUMBER** *(Include Area Code)* (937) 255-8494

Standard Form 298 (Rev. 8-98)
Prescribed by ANSI Std. Z39-18

Tracking Control For An Overactuated Hypersonic Air-Breathing Vehicle With Steady State Constraints

David O. Sigthorsson * Andrea Serrani †

Stephen Yurkovich ‡

Department of Electrical and Computer Engineering, The Ohio State University, Columbus, OH 43210 USA

Michael A. Bolender §

David B. Doman ¶

Air Force Research Laboratory, Wright-Patterson AFB, OH 45433

The development of an air-breathing hypersonic vehicle employing scramjet propulsion is an ongoing research endeavor. Because of high velocity (>Mach 5), length and positioning of the engine, and relative sleekness, the flexibility of the vehicle is significant and there are strong couplings between thrust and pitch . As a result, control design for such a vehicle is a challenge. In previous works, linear controllers have been designed for a model of the longitudinal dynamics of a specific air-breathing vehicle possessing the same number of inputs and outputs. In this paper we consider a control design for the same vehicle model, but we restrict our attention to controlling only two outputs, namely the altitude and velocity, while we employ as control inputs, the elevator deflection, total temperature change across the combustor and the diffuser area ratio of the combustor. The specific control problem addressed in the paper is the design of a controller that ensures asymptotic tracking of altitude and velocity reference trajectories, while using the redundancy in the inputs to optimize the performance in steady-state. As a matter of fact, since the system is not square, the steady state solutions that enforce perfect tracking are nonunique. The controller employs a parameterization of all possible steady state trajectories that is used for optimization of the steady state input while providing perfect tracking and fulfilment of constraint on the magnitude of the control input. Simulations results are provided to validate the proposed approach.

I. Introduction

Hypersonic air-breathing vehicles have been proposed as a promising technology for reducing the cost of launching small satellites or other vehicles into low earth orbit. Furthermore the technology may present the Air Force with efficient aircrafts capable of rapid global response. Successful progress has been made with hypersonic aircrafts such as NASA's X-43A scramjet research aircraft, which has set new Guinness world records for jet-powered aircraft speed three times in a row, reaching speeds up to Mach 9.6.[1]

Modeling of hypersonic air-breathing vehicles is a subject of active ongoing research.[2–4] Most efforts have been concentrated on modeling only the longitudinal dynamics since they present a number of challenges by themselves, especially due to strong coupling between propulsive and aerodynamic effects. Since modeling is still in its early stages, there are very few papers that have been published on the guidance and control of such aircrafts. Aside from the work by Schmidt and Velapoldi[5] and Groves et al.[6] which focuses specifically on a air-breathing vehicle model, the largest body of work done in this area regards the control of a generic

*Graduate Student, Department of Electrical and Computer Engineering, 2015 Neil Ave. Suite 205, Member IEEE

†Assistant Professor, Department of Electrical and Computer Engineering, 2015 Neil Ave. Suite 205, Member IEEE

‡Professor, Department of Electrical and Computer Engineering, 2015 Neil Ave. Suite 205, IEEE Fellow

§Aerospace Engineer, AFRL/VACA, 2210 Eighth St. Suite 21, Senior Member AIAA

¶Senior Aerospace Engineer, AFRL/VACA, 2210 Eighth St. Suite 21, Senior Member AIAA

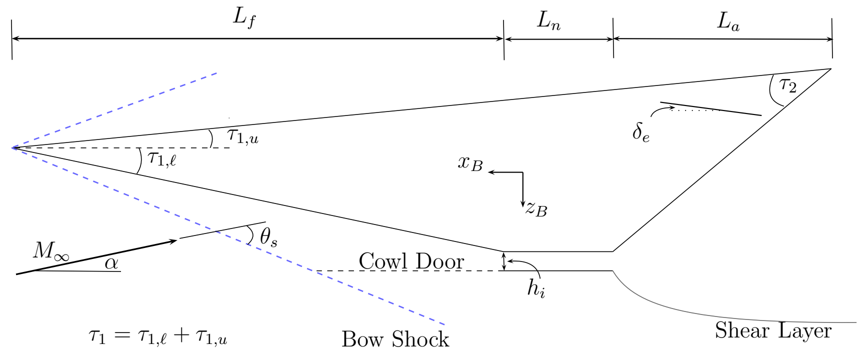

Figure 1. Vehicle Geometry for Hypersonic Air-breathing Vehicle from Bolender and Doman[2]

hypersonic vehicle models (for instance, see the robust nonlinear controllers proposed by Marrison, et al.[7] and the adaptive sliding mode controller by Xu, et al.[8]).

As can be expected, controlling air-breathing hypersonic vehicles is a difficult task. Even after linearization of the dynamics, control challenges are still present such as instability, weak controllability of some modes, considerable coupling between modes, and potential over actuation depending on input and output selection.

We will focus on control system design for the model developed by Bolender and Doman[2] which has been previously used in Ref.6. The plant model has three inputs, namely the total temperature change across the combustor, elevator deflection, and diffuser area ratio. As opposed to the case considered in Ref.6, where the outputs to the be controlled were the vehicle speed, angle of attack and altitude, we consider in this paper the problem of controlling speed and altitude only. Thus in the case considered here we have an overactuated system and input trajectories that provide perfect tracking are non-unique.

When considering an overactuated system it is implied that for output tracking there is an input redundancy. This redundancy can be used for optimization and potentially for satisfying constraints. Traditionally this redundancy has been dealt with using optimal control or control allocation.[9–13] In this paper, we propose a different approach, which has been inspired by the work of Johansen and Sbarbaro.[14] Using an exosystem to generate the reference trajectories to be tracked, the tracking control problem is cast as a regulation problem. By parameterizing all solutions to the regulator equations,[15] we separate the control design into a design of a steady state controller and a stabilizing controller. Those two controllers can be considered separately, e.g. using state feedback and optimizing the steady state behavior of the system parameterizing the steady state trajectory. Furthermore, we can exploit this parameterization to keep the input within given constraints at steady state.

The paper is organized as follows: Section II introduces the model of the air-breathing hypersonic vehicle. In Section III the tracking problem is introduced and all solutions of the Francis equation are parameterized for an overactuated system, thus providing separation of steady state and stabilizing controllers. Sections IV, presents an optimizing steady state controller, and in Section V constraints are applied to the steady state. Finally, in Section VI simulation results are presented, and conclusions are discussed in Section VII.

II. The Model of the air-breathing Hypersonic Vehicle

The model of longitudinal dynamics of an air-breathing hypersonic vehicle we consider in this paper has been developed by Bolender and Doman[2] and used for control design in Ref.6 . Compressible flow theory was used to determine pressure and shock angles, a model of a two cantilever beam was used to model the flexible modes, and Lagrange's equations equations were used to derive the equations of motion. Figure 1 shows the vehicle geometry used for the model. The following set of equations are the non-linear equations of motion,

$$\dot{V}_t = \frac{1}{m}(F_T \cos\alpha - F_D) - g\sin(\theta-\alpha) \quad (1)$$

$$\dot{\alpha} = \frac{1}{mV_t}(-F_T \sin\alpha - F_L) + Q + \frac{g}{V_t}\cos(\theta-\alpha) \quad (2)$$

$$I_{yy}\dot{Q} = M + \widetilde{\psi}_1\ddot{\eta}_1 + \widetilde{\psi}_2\ddot{\eta}_2 \quad (3)$$

$$\dot{h} = V_t \sin(\theta-\alpha) \quad (4)$$

$$\dot{\theta} = Q \quad (5)$$

$$k_1\ddot{\eta}_1 = -2\zeta_1\omega_1\dot{\eta}_1 - \omega_1^2\eta_1 + N_1 - \widetilde{\psi}_1\frac{M}{I_{yy}} - \frac{\widetilde{\psi}_1\widetilde{\psi}_2\ddot{\eta}_2}{I_{yy}} \quad (6)$$

$$k_2\ddot{\eta}_2 = -2\zeta_2\omega_2\dot{\eta}_2 - \omega_2^2\eta_2 + N_2 - \widetilde{\psi}_2\frac{M}{I_{yy}} - \frac{\widetilde{\psi}_2\widetilde{\psi}_1\ddot{\eta}_1}{I_{yy}} \quad (7)$$

where $V_t,\ \alpha,\ Q,\ h,\ \theta$ and η_i are the speed, angle-of-attack, pitch rate, altitude, pitch angle and i^{th} generalized elastic coordinates respectively, $F_T,\ F_L,\ F_D,\ N_1$, and N_2 are the trust, lift, drag, and i^{th} generalized elastic forces respectively, M is the pitching moment about the y-axis, I_{yy} is the moment of inertia, and $\zeta_i,\ \omega_i$ are the i^{th} damping coefficient and natural frequency of the elastic modes. Also,

$$\begin{array}{lll} k_1 = 1 + \frac{\widetilde{\psi}_1}{I_{yy}}, & & \widetilde{\psi}_1 = \int_{-L_1}^{0} \dot{m}_1\epsilon\phi_1(\epsilon)d\epsilon, \\ k_2 = 1 + \frac{\widetilde{\psi}_2}{I_{yy}}, & & \widetilde{\psi}_2 = \int_{-L_2}^{0} \dot{m}_2\epsilon\phi_2(\epsilon)d\epsilon \end{array} \quad (8)$$

where $\dot{m}_1,\ \dot{m}_2$ are the mass densities of the forebody and aftbody respectively, and $\phi_1,\ \phi_2$ are the mode shapes for the forebody and aftbody respectively. The states and inputs are given in Table 1. The control inputs are the total temperature change across the combustor ΔT_0, elevator deflection δ, and diffuser area ratio A_d. The inputs affect the forces and moments which in turn affect the states. As expected, ΔT_0 and A_d greatly affect the velocity and δ mainly affects the angle-of-attack and pitch. However, there exist strong couplings that can not be ignored which are caused largely by the high operating velocity of the vehicle, the positioning of the engine, and the flexible effects.

Among the possible output choices, in this paper we use the vehicle altitude and speed as outputs to be regulated, i.e. we wish to have the speed and altitude track a desired reference trajectory.

The full non-linear model is very complex and thus does not lend itself to a model based control design. For our design we will therefore consider a linearized model which was found using numerical methods to linearize the non-linear model around a trim condition, which is the one given in Table 2. The linearized model is expressed in the usual form

$$\dot{x}_p = A_p x_p + B_p u_p \quad (9)$$

$$y_p = C_p x_p, \quad (10)$$

with state $x_p \in \mathbb{R}^9$, input $u_p \in \mathbb{R}^3$ and output $y_p \in \mathbb{R}^2$. For that specific trim condition, the linearized model

States		**Inputs**	
V_t	Vehicle speed - Output	δ_e	Control surface deflection
α	Angle-of-attack	ΔT_0	Total temperature change across combustor
Q	Pitch rate	A_d	Diffuser area ratio
h	Altitude - Output	x_d	Cowl lip position (Fixed at trim)
θ	Pitch angle		
η_i	Generalized elastic coordinates		
$\dot{\eta}_i$	Generalized elastic coordinates time derivatives		

Table 1. Definitions of the states, outputs and inputs for the hypersonic air-breathing vehicle modeled in Ref.2

States at Trim:		Inputs at Trim:
V_t = 7846.4 ft/sec	η_1 = 1.6105	δ_e= 7.8589°
α = 1.9605°	$\dot{\eta}_1$ = 0	ΔT_0= 484.49 degR
Q = 0 deg/sec	η_2 = 1.4582	A_d= 0.35
h = 85000 ft	$\dot{\eta}_2$ = 0	x_d=7.0967 fixed
θ = 1.9605°		

Table 2. Trim condition for the inputs and states of the nonlinear hypersonic air-breathing vehicle model.

has no transmission zeros and the eigenvalues of the A matrix, i.e. the poles of the plant, are

$$[-0.392 \pm 20.1i,\ -0.320 \pm 16.4i,\ 0.811,\ -0.881,\ -1.91 * 10^{-4},\ -4.63 * 10^{-5} \pm 0.0399i].$$

In order to fulfill actuator bandwidth constraints we append to the plant a simple model of the actuator dynamics, given by

$$\dot{x}_\delta = A_\delta x_\delta + B_\delta u_\delta, \tag{11}$$

where

$$A_\delta = \begin{pmatrix} -20 & 0 & 0 \\ 0 & -10 & 0 \\ 0 & 0 & -10 \end{pmatrix},\ B_\delta = \begin{pmatrix} 20 & 0 & 0 \\ 0 & 10 & 0 \\ 0 & 0 & 10 \end{pmatrix},\quad x_\delta = \begin{pmatrix} x_{\delta_e} \\ x_{\Delta T_0} \\ x_{A_d} \end{pmatrix},\quad u_\delta = \begin{pmatrix} u_{\delta_e} \\ u_{\Delta T_0} \\ u_{A_d} \end{pmatrix}.$$

The resulting augmented system is written as

$$\begin{aligned} \dot{x} &= Ax + Bu \\ y &= Cx, \end{aligned} \tag{12}$$

where

$$A = \begin{pmatrix} A_p & B_p \\ 0 & A_\delta \end{pmatrix},\quad B = \begin{pmatrix} 0 \\ B_\delta \end{pmatrix},\quad C = \begin{pmatrix} C_p & 0 \end{pmatrix},\quad x = \begin{pmatrix} x_p \\ x_\delta \end{pmatrix},\quad u = u_\delta.$$

The linear system with states x, input u and output y will be referred to as the linear model of the air-breathing hypersonic vehicle. This is the model that we will use for our control design in the sequal.

III. The Tracking Problem

The linear regulator problem is a fundamental problem in modern control which models a variety of control applications. Specifically, the output regulation problem consists in letting the output of a system track a reference trajectory or rejecting a disturbance generated by an autonomous LTI system. The conditions for existence of a solution of the regulator problem can be summarized by two conditions: stabilizability of the system and solvability of the so-called Francis equations.[15–17]

To set up the tracking problem that will be investigated in this paper, let us consider the linear system

$$\begin{aligned} \dot{x} &= Ax + Bu \\ y &= Cx, \end{aligned} \tag{13}$$

where $x \in \mathbb{R}^n$, $y \in \mathbb{R}^p$, and $u \in \mathbb{R}^m$ represent the state, output, and control input respectively. The reference trajectory to be tracked $r \in \mathbb{R}^p$ is generated by an exosystem of the form,

$$\begin{aligned} \dot{w} &= Sw \\ r &= Qw \end{aligned} \tag{14}$$

where $w \in \mathbb{R}^q$ represents the exosystem state and a tracking error $e \in \mathbb{R}^p$ is defined as

$$e = y - r = Cx - Qw \tag{15}$$

In what follows, we consider the case in which the plant model (13) is over-actuated, that is $m > p$.

Definition III.1 (Tracking Problem) *The tracking problem for (13) and (14) consists in finding a control law such that*

- *The origin of (13) is asymptotically stable when* $w(t) \equiv 0$.
- *For any initial conditions of the system and exosystem the tracking error (15) converges asymptotically to 0.*

The full information tracking problem assumes that $x(t)$ and $w(t)$ are available for feedback and the control input u is given by,

$$u = -Kx + Lw, \tag{16}$$

where $K \in \mathbb{R}^{m\times n}$ and $L \in \mathbb{R}^{m\times q}$. The full information tracking problem is formally defined as follows.

Definition III.2 (Full Information Tracking Problem) *Given* $\{A, B, C, S, Q\}$ *find* $K \in \mathbb{R}^{m\times n}$ *and* $L \in \mathbb{R}^{m\times q}$ *such that*

- *(A-BK) is Hurwitz.*
- *For any initial condition, the trajectory of*

$$\begin{aligned} \dot{x} &= (A - BK)x + BLw \\ \dot{w} &= Sw \end{aligned} \tag{17}$$

satisfies $\lim_{t\to\infty} ||Cx(t) - Qw(t)|| = 0$

Theorem III.1 below due to Francis, gives the conditions for the solvability of the problem in terms of the existence of a solution to a certain linear matrix equation.[15,17]

Theorem III.1 *The full information tracking problem is solvable iff:*

1. (A, B) *is stabilizable*
2. $\exists$ *matrices* $\Pi \in \mathbb{R}^{n\times q}$ *and* $\Gamma \in \mathbb{R}^{m\times q}$, *solutions of the Francis equation*

$$\begin{aligned} \Pi S &= A\Pi + B\Gamma \\ 0 &= C\Pi - Q. \end{aligned} \tag{18}$$

The condition that (A, B) is stabilizable can be tested using standard techniques.[18] The solvability of the Francis equations is more involved. For our study, we will make use of Theorem III.2 which gives a sufficient condition for its solvability.[16,17]

Theorem III.2 *If*

$$\operatorname{rank}\begin{pmatrix} A - \lambda I & B \\ C & 0 \end{pmatrix} = n + p, \tag{19}$$

for any $\lambda \in \operatorname{spec}(S)$, *then the Francis equations (18) are solvable for any* Q.

The solution of the Francis equation defines the steady state of the system on which the tracking error is identically zero, and the input required to maintain the system in steady state. This steady state solution can be expressed in terms of solutions of the Francis equations as

$$x^{\mathrm{ss}} = \Pi w, \quad u^{\mathrm{ss}} = \Gamma w. \tag{20}$$

The next issue we need to address is to design a controller that steers the trajectories of the system to the steady state. Consider the following change of coordinates

$$\widetilde{x} = x - x^{\mathrm{ss}}, \qquad \widetilde{u} = u - u^{\mathrm{ss}}. \tag{21}$$

By substitution into equations (13) and (15) we can express the dynamics and tracking error in the new coordinates as

$$\begin{aligned} \dot{\widetilde{x}} &= A\widetilde{x} + B\widetilde{u} \\ e &= C\widetilde{x}. \end{aligned} \tag{22}$$

Observe that by construction if $\widetilde{x}(t) = 0$ then the state and input is equal to the steady state solution (20) and the tracking error is identically zero. Thus, to solve the tracking problem we need to stabilize the origin of equation (22). This is achieved by means of state feedback choosing a feedback gain $K \in \mathbb{R}^{m\times n}$ such that $(A - BK)$ is Hurwitz and by applying the control law

$$\widetilde{u} = -K\widetilde{x}. \tag{23}$$

The application of the control law (23) renders the steady state solution x^{ss} given by the first identity in (20) attractive, while the conditions of Definition III.2 are satisfied by construction. Note that the choice of a steady state control is completely independent from the choice of a stabilizing control law. This separation is key for the methods we will develop for steady state optimization in later sections.

Combining the steady state with the stabilizing control, we can express the control law as

$$u \quad = \quad u^{\text{ss}} + \widetilde{u} \quad = \quad \Gamma w - K(x - \Pi w) \quad = \quad -Kx + (\Gamma + K\Pi)w. \tag{24}$$

By comparing this resulting control law to Definition III.2 we observe that the feedforward gain can be written as $L = (\Gamma + K\Pi)$.

A. Solving the Over-Actuated Tracking Problem

It is shown in Ref.15 that if Theorem III.2 holds for a square system ($m = p$), then the solution of the Francis equations is unique. If the system is over actuated ($m > p$) then the solution is in general not unique. In this case, we seek to find all solutions to the Francis equations and parameterize them. This parameterization can then be utilized for steady state optimization and satisfying constraints on the steady state.

We start rewriting equations (18) as

$$\underbrace{\begin{pmatrix} 0 \\ Q \end{pmatrix}}_{R} = \underbrace{\begin{pmatrix} A & B \\ C & 0 \end{pmatrix}}_{A_1}\underbrace{\begin{pmatrix} \Pi \\ \Gamma \end{pmatrix}}_{X} - \underbrace{\begin{pmatrix} I & 0 \\ 0 & 0 \end{pmatrix}}_{A_2}\underbrace{\begin{pmatrix} \Pi \\ \Gamma \end{pmatrix}}_{X} S$$

or

$$R = A_1X - A_2XS. \tag{25}$$

Equation (25) is a special case of the so-called Hautus matrix equations.[17] For brevity let us denote the dimensions of the matrices X and R as $\bar{m}$ and $\bar{p}$, respectively, i.e., let

$$\bar{m} := \dim(X) = (n + m)q, \qquad \bar{p} := \dim(R) = (n + p)q, \qquad \bar{m} > \bar{p}. \tag{26}$$

We introduce the mapping

$$\mathcal{H} : \mathbb{R}^{\bar{m}} \mapsto \mathbb{R}^{\bar{p}}, \qquad \mathcal{H}(X) = A_1X - A_2XS, \tag{27}$$

so equation (25) can represented as $\mathcal{H}(X) = R$. If the conditions of Theorem III.2 hold, then $\mathcal{H}$ is onto, which implies that the equation $\mathcal{H}(X) = R$ is always solvable for any $R \in \mathbb{R}^{\bar{p}}$. In order to find an algebraic solution to the equation $\mathcal{H}(X) = R$, we express it as the linear system of equations

$$H\mathbf{x} = \mathbf{r} \tag{28}$$

where the $H \in \mathbb{R}^{\bar{p}\times\bar{m}}$, $\mathbf{x}$ and $\mathbf{r}$ are defined as

$$H = I_{q\times q} \otimes A_1 - S^{\mathrm{T}} \otimes A_2, \qquad \mathbf{x} = \mathrm{col}(X), \qquad \mathbf{r} = \mathrm{col}(R), \tag{29}$$

where the symbol $\otimes$ denotes the Kronecker product, and $\mathbf{x} \in \mathbb{R}^{\bar{m}}$ and $\mathbf{r} \in \mathbb{R}^{\bar{p}}$ are tall vectors constructed from the column vectors of X and R respectively. The matrix $H \in \mathbb{R}^{\bar{p}\times\bar{m}}$ has rank $\bar{p}$ by assumption. Every solution of equation (28) can be expressed as

$$\mathbf{x} = \mathbf{x}^p + \mathbf{x}^0 \tag{30}$$

where $\mathbf{x}^p \in \mathbb{R}^{\bar{m}}$ is a particular solution, and $\mathbf{x}^0 \in \ker(H)$. Let $\bar{q}$ denote the dimension of the kernel of H, i.e.

$$\bar{q} := \dim(\ker(H)) = \dim(X) - \dim(R) = \bar{m} - \bar{p}. \tag{31}$$

From equation (30) it is evident that there exists an infinite number of solutions to equation (28) and the dimension of the solution space is precisely $\bar{q}$. This observation leads us to Proposition III.3.

Proposition III.3 *Assuming that $H \in \mathbb{R}^{\bar{p}\times\bar{m}}$ in (28) has rank $\bar{p}$, then there exist $\bar{q}$ linearly independent vectors such that $\mathbf{x}^0$ in (30) can be expressed as*

$$\mathbf{x}^0 = \mathbf{k}_1\theta_1 + \mathbf{k}_2\theta_2 + \cdots + \mathbf{k}_{\bar{q}}\theta_{\bar{q}}, \qquad \textit{where} \quad \theta_i \in \mathbb{R},\ i = 1, \ldots, \bar{q} \tag{32}$$

The proof of Proposition III.3 follows elementary arguments. In particular, the set of vectors $\{\mathbf{k}_i\}$ is any set of linearly independent vectors spanning $\ker(H)$. Using equation (32) we can write the solution of equation (25) as

$$\begin{pmatrix} \Pi \\ \Gamma \end{pmatrix} = X = X^{\mathrm{p}} + X^0 \tag{33}$$

where the column vectors of X^{p} and X^0 can be found from $\mathbf{x}^{\mathrm{p}}$ and $\mathbf{x}^0$, respectively. Therefore, analogously to Proposition III.3, there exists $\bar{q}$ linearly independent matrices $N_1,\ N_2,\ \ldots,\ N_{\bar{q}} \in \mathbb{R}^{(n+m)\times q}$ spanning $\ker(\mathcal{H})$ such that

$$X^0 = N_1\theta_1 + N_2\theta_2 + \cdots + N_{\bar{q}}\theta_{\bar{q}}. \tag{34}$$

To recap, we now have our expression for all matrices Π and Γ that satisfy the Francis equations, parameterized by $\theta \in \mathbb{R}^{\bar{q}}$ as in (34), where θ is an arbitrary constant vector. Therefore, with a slight abuse of notation justified by the linearity of the parameter θ, we can write the steady state solutions as

$$\begin{array}{ccccccc} x^{\mathrm{ss}} & = & \Pi w & = & \Pi^{\mathrm{p}} w + \Pi(\theta) w & = & \Pi^{\mathrm{p}} w + \Pi(w)\theta \\ u^{\mathrm{ss}} & = & \Gamma w & = & \Gamma^{\mathrm{p}} w + \Gamma(\theta) w & = & \Gamma^{\mathrm{p}} w + \Gamma(w)\theta. \end{array} \tag{35}$$

The control law can be expressed as

$$u \quad = \quad -Kx + (\Gamma^p + \Gamma(\theta) + K(\Pi^p + \Pi(\theta)))w. \tag{36}$$

where $K \in \mathbb{R}^{m\times n}$ is the stabilizing feedback, and $\theta \in \mathbb{R}^{\bar{q}}$ is an arbitrary constant vector that defines a particular steady state solution.

IV. Optimization

In this section, we employ optimization methods to choose the value of the parameter vector θ. The optimization objective is to minimize a given cost function on a moving horizon given by the time interval between the knot points of a reference spline trajectory, generated by a suitable exosystem.

The cost function we will consider depends on the integral of the steady state input over a given time interval and the squared 2-norm of the difference between θ and the optimal choice of θ for the previous time interval. We will consider both an offline and an online approach to solve the optimization problem. When using an offline approach, the optimal constant θ is computed for a given time interval during the previous one. To apply the optimal θ, the value of the parameter vector θ is simply switched at the start of each interval. When using an online approach, dynamics are assigned to θ such that during each given time interval, θ converges continuously to the offline optimal θ.

A. Problem Formulation

The system that we will consider is defined in Section III by equations (13) through (15), with the assumption of over-actuation, $m > p$, and that the full information tracking problem is solvable. The following assumptions define the class of reference trajectories generated by the exosystem (14).

Assumption IV.1 *The exosystem in (14) generates cubic splines as reference trajectories for each output of the system in (13).*

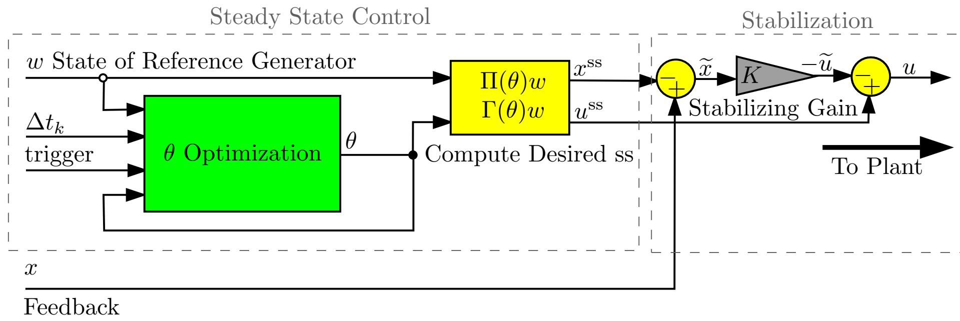

Figure 2. Controller Structure (the "trigger" is a trigger signal sent at $t = t_k$ for each $k \in \mathbb{N}$)

Assumption IV.2 *There exist a time $T > 0$ such that for all $k \in \mathbb{N}$ the time interval $[t_k, t_{k+1})$ between spline knot points is such that $(t_{k+1} - t_k) \geq T$.*

Assumption IV.1 is fulfilled using a chain of integrators and resetting the initial conditions at the knot points of the splines. The purpose of Assumption IV.2 is to ensure that there is enough time to complete the steady state optimization computations for the next time interval. By choosing T large enough, we also ensure that if θ is changed at the beginning of a time interval, the stabilizer will have sufficient time to let the trajectories of the system converge to the steady state before the end of the interval. In the actual implementation, this will be achieved by tuning T, the stabilizing gain, the rate of convergence of θ to the offline optimal θ (for an online approach), and the weights in the cost function.

Let θ_k be the constant steady state parameter θ over the $k^{\rm th}$ time interval between the $k^{\rm th}$ and $(1+k)^{\rm th}$ reference spline knot points, i.e.

$$\theta(t) = \theta_k, \quad \forall t \in [t_k, t_{k+1}). \tag{37}$$

We will consider a scalar cost function $J_k(\theta_k) : \mathbb{R}^{\bar{q}} \mapsto \mathbb{R}$ defined over the $k^{\rm th}$ interval between the reference spline knot points. For each time interval, we desire to find the value θ_k^*, such that the given cost function $J_k(\theta_k)$ is minimized, i.e.

$$\theta_k^* = \arg\min_{\theta_k} J_k(\theta_k) \tag{38}$$

The cost function we will consider is intended to penalize the input energy at steady state over the given time interval, while also weighting the change of θ_k in squared 2-norm.

The cost function is chosen as

$$J_k = \frac{\alpha_1}{\Delta t_k} \int_{t_k}^{t_k+1} u^{\rm ss}(w^k, \theta_k, \tau)^{\rm T} u^{\rm ss}(w^k, \theta_k, \tau) d\tau + \frac{\alpha_2}{\Delta t_k} |\theta_k - \theta_{k-1}^*|^2 \tag{39}$$

where $\alpha_1 \in \mathbb{R}$ and $\alpha_2 \in \mathbb{R}$ are positive weighting parameters, $\Delta t_k = (t_{k+1} - t_k)$, and the steady state input over $t \in [t_k, t_{k+1})$ resulting from the choice $\theta = \theta_k$ is written as

$$u^{\rm ss}(w^k, \theta_k, t) = (\Gamma^{\rm p} + \Gamma(\theta_k)) e^{S(t-t_k)} w^k, \tag{40}$$

where $w^k = w(t_k)$. Obviously by increasing the ratio α_2/α_1 we will reduce the change in norm between θ_k^* and θ_{k-1}^*. However, we want to avoid choosing α_2/α_1 large since our main objective is to minimize the steady state input energy.

We will solve the optimization problem in equation (38) with an offline approach and an online approach for both unconstrained and constrained optimization to enforce constraints on the input at steady state. The offline approach refers to changing θ in discrete steps as the exosystem is reset, and by online we refer to assigning dynamics to $\theta(t)$ such that $\theta(t)$ converges continuously to the offline optimal θ_k^*.

The structure we seek to implement is depicted in Figure 2. Notice the distinct separation between the steady state control or design and the stabilization, this results from the specific formulation of the problem.

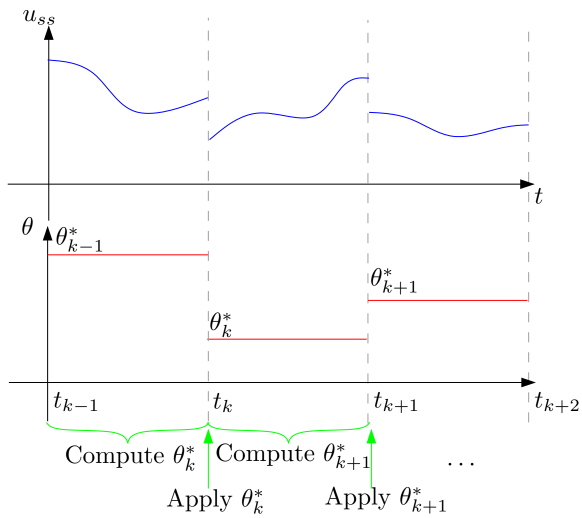

Figure 3. Simplified conceptual example for offline optimization of θ.

B. Offline Approach

The offline approach to unconstrained optimization of the given cost function J_k involves determining the optimal θ^*_k over each time interval of the reference spline and applying it by changing θ in a discrete-time fashion. Figure 3 illustrates this idea and also points out that switching θ induces discrete changes in the steady state control, and thus switching in $u^{\text{ss}}(t)$ will induce transients in $u(t)$.

To achieve unconstrained offline optimization of (39) we note that J_k given in (39) is convex in u^{ss}, and u^{ss} depends linearly on θ. The minimizer θ^*_k is found solving $\nabla_{\theta_k} J_k(\theta^*_k) = 0$, where $\nabla_{\theta_k} J_k$ denotes the gradient of J_k with respect to θ_k. To see why this is the case, we compute the gradient,

$$\nabla_{\theta_k} J_k = L_k + R_k \theta_k, \tag{41}$$

where

$$L_k = \frac{\alpha_1}{\Delta t_k} \int_{t_k}^{t_{k+1}} \Gamma^{\mathrm{T}}(w) \Gamma_p w d\tau - \frac{\alpha_2}{\Delta t_k} \theta^*_{k-1}, \qquad R_k = \frac{\alpha_1}{\Delta t_k} \int_{t_k}^{t_{k+1}} \Gamma^{\mathrm{T}}(w) \Gamma(w) d\tau + \frac{\alpha_2}{\Delta t_k} I_{\bar{q}}. \tag{42}$$

To solve $\nabla_{\theta_k} J_k(\theta^*_k) = 0$, we simply need to find the inverse of R_k, and obtain

$$\theta^*_k = -R_k^{-1} L_k. \tag{43}$$

Since $\alpha_2 > 0$, and R_k is formed by α_2 times the identity matrix, plus a positive semi-definite matrix resulting from the integration of a matrix times its transpose, then R_k is positive definite. Hence, R_k^{-1} is guaranteed to exist. Furthermore, since $R_k > 0$ then the Hessian of $J_k(\theta_k)$ with respect to θ_k is positive definite, thus θ^*_k is the global minimizer of the cost function.[19] We therefore have a valid solution to the unconstrained offline optimization problem and the solution is expressed by equation (43).

C. Online Approach

Motivated by the need to reduce the transient behavior that can occur in the control input and the plant output as a result of switching, we desire to take an approach to change θ continuously. We solve the problem by assigning dynamics to $\theta_k(t)$ such that $\theta_k(t)$ rapidly converges to the offline optimal θ^*_k. Consider the gradient-based update law

$$\dot{\theta}_k = -\gamma \nabla_{\theta_k} J_k, \quad t \in [t_k, t_{k+1}), \tag{44}$$

where $\gamma > 0$ is a design parameter. Recall that the cost function J_k changes for each time interval, which makes the gradient-based update law change discretely at the time of each reference spline knot point. We will show that this choice of $\theta_k(t)$ dynamics renders θ^*_k an asymptotically stable equilibrium, while the gain

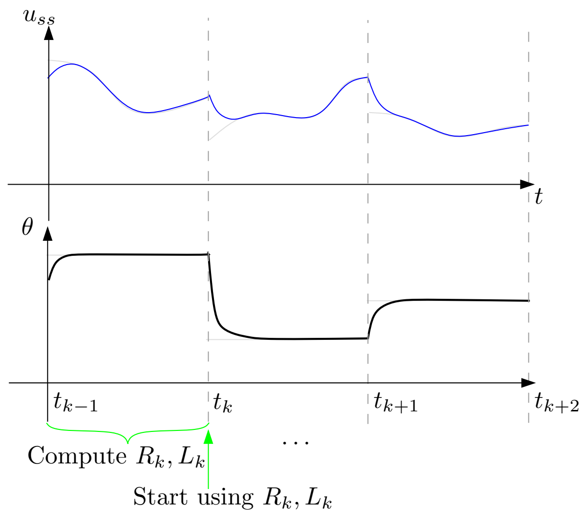

Figure 4. Simplified conceptual example for online optimization of θ.

γ affects the convergence rate of $\theta_k(t)$ to θ_k^*. To show this we start by defining the following change of coordinates

$$\widetilde{\theta}_k = \theta_k - \theta_k^*. \tag{45}$$

Recall that by definition $(L_k + R_k\theta_k^*) = 0$ and therefore the dynamics in the new coordinates can be expressed as

$$\dot{\widetilde{\theta}}_k = -\gamma R_k \widetilde{\theta}_k. \tag{46}$$

Note that since $R_k > 0$, then $-\gamma R_k$ has all negative eigenvalues and $\widetilde{\theta} = 0$ is an asymptotically stable equilibrium. Furthermore, γ scales the eigenvalues of $-\gamma R_k$ and thus the rate of convergence of θ_k to θ_k^* is proportional to γ.

Figure 4 shows in a simplified way how using a continuous $\theta(t)$ will produce a continuous $u^{\mathrm{ss}}(t)$, which will help reduce transients in $u(t)$.

V. Constrained Optimization

It is well known that in most control applications there are constraints on the states and inputs of the system to be controlled and the air-breathing hypersonic vehicle is certainly no exception. In this section, we will add constraints to the steady state input for the system we are considering. In particular, we formulate our criteria as follows:

- Satisfy possibly asymmetric constraints on some or all of the inputs at steady state (u_i^{ss})
- Minimize the energy of the input at steady state, as a secondary objective.

We will assume that it is possible to satisfy this criteria. That assumption is made for illustrative purposes that the constrained problem fits directly into our framework. To simplify the problem, we will consider only a constraint on one of the inputs, the i^{th} input. An offline and an online approach will be considered. Since the online approach utilizes the results of the offline approach, the online approach is more aptly referred to as an online extension.

First, we need to set up some assumptions, notation and terminology. We define constraints on the i^{th} input at steady state as follows: given scalars $\underline{u} < \bar{u}$, we desire a control at steady state u^{ss} such that

$$u^{\mathrm{ss}} \in \mathcal{U}, \text{ where } \mathcal{U} = \{u^{\mathrm{ss}} \in \mathbb{R}^m : \underline{u} \leq u_i^{\mathrm{ss}} \leq \bar{u}\}, \tag{47}$$

where u_i^{ss} denotes the i^{th} steady state input. We define $\theta_k(t)$ to be a feasible parameter trajectory at time $t \in [t_k, t_{k+1})$ if $\underline{u} < u_i^{\mathrm{ss}}(w^k, \theta_k, t) < \bar{u}$. Furthermore, let us define the set Θ_k as

$$\Theta_k = \{\theta : \underline{u} < u_i^{\mathrm{ss}} < \bar{u},\ u^{\mathrm{ss}} = (\Gamma_p + \Gamma(\theta))e^{S(t-t_k)}w^k,\ \forall t \in [t_k, t_{k+1}].\} \tag{48}$$

and refer to Θ_k as the feasible parameter set over the time interval $[t_k, t_{k+1})$. Note that even though $\mathcal{U}$ is not time varying, the boundary $\partial\Theta_k$ of the feasible set Θ_k does in general vary between time intervals. Also note that by continuity $\theta_k \in \Theta_k$ implies that for some $t_\varepsilon > 0$, $\theta_k(t)$ is feasible over $[t_{k+1}, t_{k+1} + t_\varepsilon)$. We will assume that Assumptions IV.1 and IV.2 still hold. In addition, we assume that there is sufficient control authority to solve the constrained optimization problem:

Assumption V.1 *Given the full information tracking problem as described in Section III,* $\forall k \in \mathbb{N}$, $\exists\, \theta_k \in \Theta_k$ *and a scalar* $\varepsilon > 0$ *such that* $(\underline{u} + \varepsilon) < u_i^{\mathrm{ss}}(\theta_k, t) < (\bar{u} - \varepsilon)$, $\forall\, t \in [t_k,\ t_{k+1}]$.

The constrained problem can now be expressed as finding the optimal θ_k^* over the k^{th} time interval such that

$$\theta_k^* = \arg \min_{\theta_k \in \Theta_k} J_k(\theta_k) \tag{49}$$

where Θ_k is defined by (48) and $J_k(\theta_k)$ is defined by (39). As with the unconstrained case, we will consider both an online and an offline approach to solving this problem. We will change θ in discrete steps for the offline case and assign the dynamics of θ_k for the online case such that $\theta_k(t)$ converges to θ_k^* without becoming unfeasible at any point in time.

A. Offline Approach

The problem of finding an offline constrained optimal θ_k over the time interval $[t_k, t_{k+1}]$ will be split into two steps:

- Step 1: Find an initial guess $\theta_k^0 \in \Theta_k$ for θ_k^*.
- Step 2: With such an initial guess for the optimization, find a θ_k^* that minimizes the cost function J_k defined by (39) in the sense of (49), i.e. optimize such that $\theta_k^* \in \Theta_k$.

Since our main objective is to ensure that a given θ_k is in the feasible set Θ_k, we must have a way to test for such feasibility. Let us define a 2^{nd} order polynomial of u_i^{ss} that is negative iff u_i^{ss} is within the constraints, i.e.

$$c(u_i^{\mathrm{ss}}) \;=\; {u_i^{\mathrm{ss}}}^2 + c_1 u_i^{\mathrm{ss}} + c_0,\ \text{such that}\quad c(\underline{u}) = c(\bar{u}) = 0,\ \text{and}\ c(u_i^{\mathrm{ss}}) < 0\ \forall u_i^{\mathrm{ss}} \in \{u_i^{\mathrm{ss}} : \underline{u} < u_i^{\mathrm{ss}} < \bar{u}\}. \tag{50}$$

Since $w(t)$ is a polynomial in t then u_i^{ss} is a polynomial in t which allows us to also express $c(u_i^{\mathrm{ss}})$ as a polynomial in t i.e. $c(\tau_k)$ with a slight abuse of notation, where $\tau_k = t - t_k$. If the roots of $c(\tau_k)$ are within $[0, \Delta t_k]$, then the constraints will be violated within the k^{th} time interval. We have thus come up with a feasibility check that can also tell us at what point, or points, in time an unfeasible θ_k allows the steady state input to violate a constraint.

Our next task is to find a θ in Θ_k. We will accomplish this by using a gradient optimization technique. The method involves setting up a cost function that makes the cost small if the input is within the constraints but rapidly gets larger if the input is near or outside the constraints. Since by Assumption V.1 there exists an input that is feasible over the given time interval, then there should exist an input that makes this cost function small. First a cost function is defined as follows

$$J_\phi = \frac{1}{\Delta t_k} \int_{t_k}^{t_{k+1}} \alpha_3 \phi(u_i^{\mathrm{ss}}) d\tau \tag{51}$$

where $\alpha_3 > 0$ is a weighting gain. We choose $\phi(\cdot)$ as a convex, positive definite function with $\phi(\underline{u}) = \phi(\bar{u})$. We will use

$$\phi(u_i^{\mathrm{ss}}) = l(u_i^{\mathrm{ss}})^{2\nu},\ 0 < \nu \in \mathbb{N}, \qquad \text{where} \quad l(u_i^{\mathrm{ss}}) = \frac{2u_i^{\mathrm{ss}} - (\bar{u} + \underline{u})}{\bar{u} - \underline{u}}. \tag{52}$$

Basically we construct a line, $l(\cdot)$, that intersects -1 and 1 at $\underline{u}$ and $\bar{u}$ respectively, then $\phi(\cdot)$ is $l(\cdot)$ raised to an even power to create the desired convex function that is exactly 1 at $\underline{u}$ and $\bar{u}$. Given Assumption V.1, choosing a large enough ν guarantees that minimizing J_ϕ with respect to θ_k will result in a θ_k in Θ_k. Let t_ϕ be defined as

$$t_\phi = \min(\{t_e, t_{k+1}\}) \tag{53}$$

where t_e is such θ_k is feasible over $[t_k, t_e)$ and unfeasible at t_e if θ_k is unfeasible at any time $> t_k$, else $t_e = \infty$. Then to get a θ_k that is in Θ_k we only need to iteratively minimize J_ϕ until $t_\phi = t_{k+1}$. This is method is described by Algorithm V.2.

Algorithm V.2 (Step 1) *Let $\theta^*_{k-1} \in \Theta_{k-1}$ denote the minimizer for the previous reference spline interval. By continuity θ^*_{k-1} is feasible over at least $[t_k, t_k + t_\varepsilon)$ for some $t_\varepsilon > 0$.*

1. *Assign $\theta^0_k = \theta^*_{k-1}$. If $\theta^0_k \in \Theta_k$, do nothing and return $\theta^0_k = \theta_{k-1}$.*
2. *Otherwise, iteratively minimize J_ϕ until we get $t_\phi = t_{k+1}$, i.e. we have a θ^0_k that is in Θ_k. Return θ^0_k.*

The next thing we need to do is optimize θ over $[t_k, t_{k+1})$ without violating the constraints on u_i^{ss}. We will do this with a gradient method initialized with θ^0_k employing the same cost function as we used for the unconstrained steady state optimization, i.e. J_k from equation (39). To satisfy the constraints in an optimization algorithm we implement Algorithm V.3.

Algorithm V.3 (Step 2) *Let θ^0_k be the initial guess for θ^*_k, obtained using Algorithm V.2.*
Iteratively optimize J_k (39) (gradient method) until we

1. *Have minimized J_k to within tolerance limits, stop iterating and return θ^*_k.*
2. *Taking a step in the gradient search that is smaller in norm then a given threshold causes θ^*_k not to be in Θ_k, stop iterating and return the feasible θ^*_k without further gradient search steps.*

B. Online Extension

When dealing with the online constrained optimization, we take a different approach then the one taken for the unconstrained case. We call this an extension because we will still use the offline optimal algorithm to find a reference for θ_k. For the constrained online optimization, we will follow the following steps:

- We will assume that we have used the offline algorithm and found θ^*_k during the previous interval $[t_{k-1}, t_k)$
- Assigning $\dot{\theta}_k(t)$ to steer $(\theta_k - \theta^*_k)$ to zero, arbitrarily fast, without letting $\theta_k(t)$ become unfeasible at any time.

Recall that θ^*_{k-1} is feasible at the next interval for at least some $[t_k, t_k + t_\varepsilon]$, $t_\varepsilon > 0$. Therefore, we have at least t_ε units of time to bring $\theta_k(t)$ to a small neighborhood of θ^*_k before it becomes unfeasible ($u_i^{\mathrm{ss}}(t)$ violates its constraints).

Similarly to the online case in the unconstrained problem, we will be considering assigning a dynamics to $\theta_k(t)$ such that $\theta_k(t)$ converges to θ^*_k faster then the dynamics of the system . This assumption is made in order to justify that the changes in θ will only cause transients in the state and input that the stabilizing controller is able to render negligible within $[t_k, t_{k+1})$.

To remedy the problem of possible infeasibility during transients in $\theta_k(t)$ when using a simple feedback law in $\theta_k(t)$ as was done for the unconstrained online optimization, we suggest adding a barrier-type function to the dynamics of θ_k. Details are skipped for reasons of space, and will be given in the final version of the paper.

VI. Simulation Results

The control and optimization methods described in the previous chapters were applied to the hypersonic air-breathing vehicle model described in the Section I. The results presented in this section are mostly preliminary. Further tuning might potentially improve the results significantly. The physical meaning of the inputs has been briefly discussed in the introduction of the model but here we need to consider them in slightly more detail to make our optimization and assigning of constraints meaningful. The diffuser area ratio A_d, can obviously only vary between $[0, 1]$. We chose to use a more conservative range, $[0.14,\ 0.735]$. The range for the total temperature change across the combustor will be considered to be [500 degR, 3900 degR]. Finally, the elevator deflection should remain within the range $[-30^\circ,\ 30^\circ]$. The addition of actuator dynamics to the model takes care of the bandwidth limitation of the inputs. Because of the large differences in input ranges, we scale the B matrix to normalize their relative effect of the input on the optimization methods. The scaling factors and parameters used for the steady state optimization methods are presented in Table 3, and Table 2 shows the trim state used for the linearization of the model dynamics.

We considered four cases in our simulations:

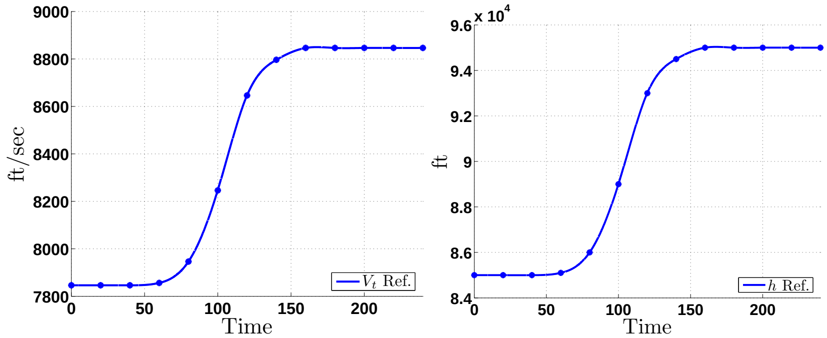

(a) Velocity Reference (b) Altitude Reference

Figure 5. Hypersonic air-breathing vehicle model: Reference for velocity and altitude.

- Offline unconstrained steady state optimization applied on the linear plant (OFF-NC-L)
- Offline constrained steady state optimization applied on the linear plant (OFF-C-L)
- Online constrained steady state optimization applied on the linear plant (ON-C-L)
- Online constrained steady state optimization on the nonlinear plant (ON-C-NL)

We applied the offline unconstrained optimization to help tune the stabilizer and get fair results while allowing A_d to violate its constraints. Then we considered the offline constrained optimization to prevent violating the constraints on A_d. The online constrained optimization was used to reduce transients in the response observed for the offline case. Finally, the online constrained optimization was applied to the nonlinear model.

For the stabilizing controller, we chose to use state feedback with a gain K as in the examples given in the previous chapters. To tune the feedback gain we use LQR methods on the linear system with the scaled B matrix and the following weighting matrices,

$$\begin{aligned} R &= I_{3\times3} \\ Q &= \mathrm{diag}(10.0,\ 10^{-3},\ 10^{-3},\ 1.0,\ 10^{-3},\ 10^{-6},\ 10^{-6},\ 10^{-6},\ 10^{-6},\ 0.0,\ 0.0,\ 0.0). \end{aligned}$$

For the unconstrained cases:					
$\alpha_1 = 1$	α_2=0.1		$\gamma = 100$		
For the constrained cases:					
$\alpha_1 = 1$	$\alpha_2 = 10$	$\gamma = 0.3$	$\underline{u}$ = -0.21	$\bar{u}$ = 0.385	constrain u_3^{ss}
$\alpha_3 = 1$	$\nu = 4$				
Input scaling factors:					
δ_e: 1/10	ΔT_0: 1/1000		A_d: 1/0.7		

Table 3. Parameters for the optimization and scaling of the inputs. The constraints are presented w.r.t. unscaled input as deviations from the trim condition and are conservative.

The reference velocity and altitude that were chosen are shown on Figure 5. We chose an approximation of a step of 1000 ft/sec in velocity and 10000 ft in altitude over time span of 93 s (within 1% of the initial and final value). Those are compatible references for velocity and altitude to the ones used in Ref.6. Figure 6 shows the tracking error, which is small with respect to the amplitude of the reference. The velocity and altitude references are of the order of 10^3 and 10^4, respectively, while the error is only 10^{-1} and 10^0 respectively. As expected, the error for the nonlinear model is greater then for the linear, but it is still very small.

Figure 7 shows u^{ss}. We observe that for the unconstrained case we grossly violate the constraints on A_d. However, we also see that all the constrained cases do not allow A_d to become unfeasible. The variations in

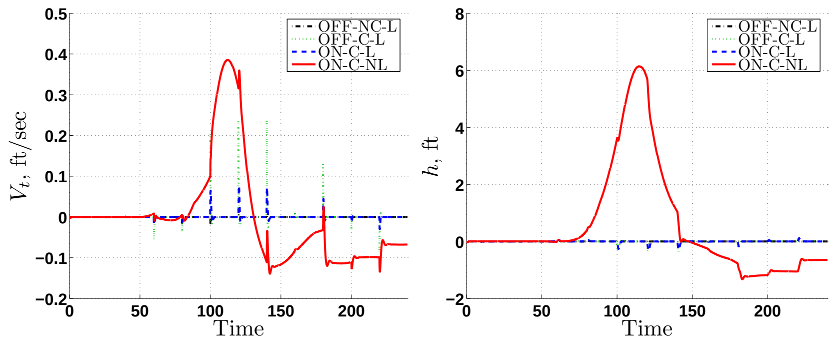

(a) Velocity Tracking Error (b) Altitude Tracking Error

Figure 6. Tracking error for velocity and altitude.

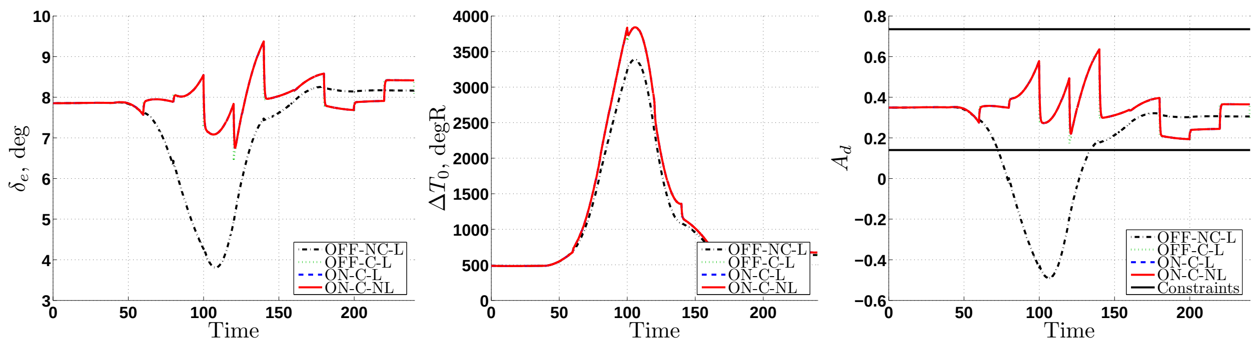

(a) δ_e^{ss} (b) ΔT_0^{ss} (c) A_d^{ss}

Figure 7. Steady state inputs ($u^{ss} = [\Gamma^{\text{p}} + \Gamma(\theta)]w(t)$+trim).

δ_e are also well within reasonable amplitudes. ΔT_0 becomes quite large but that can possibly be adjusted by further tuning. Figure 8 shows the inputs to the model of the hypersonic air-breathing vehicle, notice the transients caused by changing θ. As expected, the online approach greatly reduces the transients. In fact the transients are reduced enough that for the online cases the transients in A_d not to exceed its constraints.

Figure 9 shows θ for the cases we considered. We have an eight dimensional θ parameter so visualizing its effects directly from the graph is difficult at best. Because of this difficulty, the only comments we will make on this graph are that we observe that the different methods we use to choose θ give different results, and that the online methods give a continuous θ, while the offline methods change θ discretely. The rapid convergence of $\theta_k(t)$ for the online cases to the offline optimizer θ_k^* makes it difficult to distinguish between the two approaches on Figure 9.

Finally, we plot some of the states that are not outputs on Figure 10. The angle of attack is of great importance since the vehicle may not function if the amplitude of α becomes too large, i.e. goes outside $[-5°, 5°]$. Figure 10 shows that α remains within about 1.5° from the trim condition for the constrained cases. It does seem to make rather abrupt changes but note that the time scale is considerably long with respect to the dynamics of the system. The pitch angle it varies only up to about 2-3° from the trim which also is not great enough to cause concern. Observe also that the flight path angle (FPA) is reasonable and evolves without making abrupt changes in amplitude. Finally, the generalized flexible modes vary in amplitude no more then what was observed in Ref.6.

VII. Conclusions

The model of the air-breathing hypersonic vehicle presents a significant control challenge as was discussed in this study. Linearization was used to produce a simplification the model which yields itself better to control

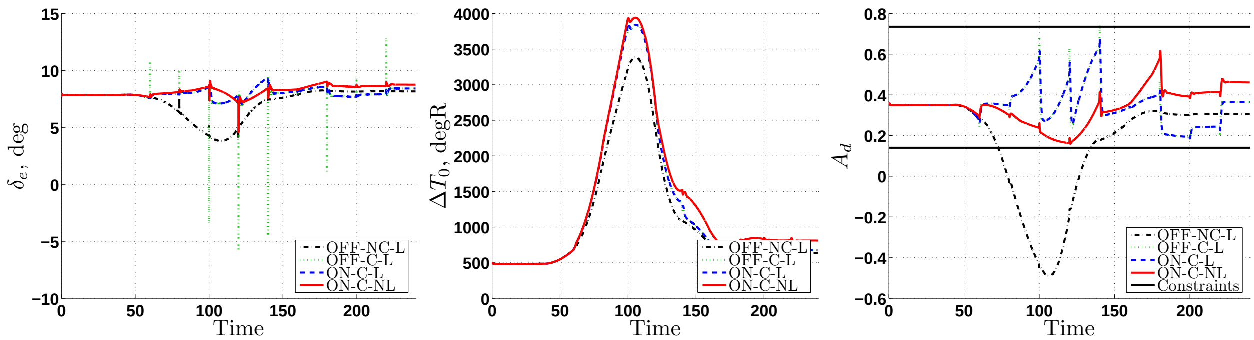

(a) δ_e (b) ΔT_0 (c) A_d

Figure 8. Inputs to the model of the hypersonic air-breathing vehicle (u_p).

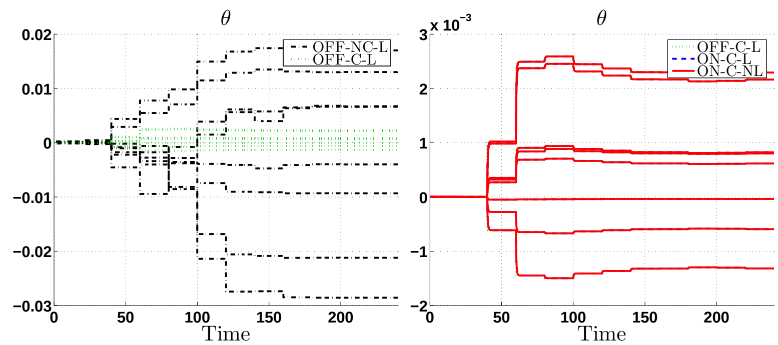

(a) θ (b) θ

Figure 9. The parameter θ for the cases under consideration.

design. A control method was presented that allows designing a steady state and a stabilizing controller separately for tracking control of this overactuated system. Using state feedback for stabilizing control and optimization methods for steady state control, both unconstrained and constrained, we were able to produce promising results in simulation. Those results show very tight tracking performance for reference trajectories that are more demanding that those presented in Ref.20. Also we showed that we were able to produce near perfect tracking under steady state input constraints even when applying the controllers to the full nonlinear model of the air-breathing hypersonic vehicle.

The work presented in this study opens up a door to further research on methods using the regulator approach to the tracking problem for over-actuated systems. Robustness analysis of the control methods, and a detailed analysis of the stability and rate of convergence for the constrained optimization methods are examples of potential research topics. We should also note that in this paper, we do not necessarily assume we have a differentially flat system, which is a standard assumption made for conventional trajectory optimization methods applied to over-actuated systems.[11,13] Finally, detailed geometric analysis of the regulator problem formulation and solution may lead to analogous approaches to non-linear control, then a new non-linear control method could potentially be developed.

VIII. Acknowledgements

This work was performed while D. O. Sigthorsson was supported by the Air Force Research Laboratory and by a DAGSI fellowship.

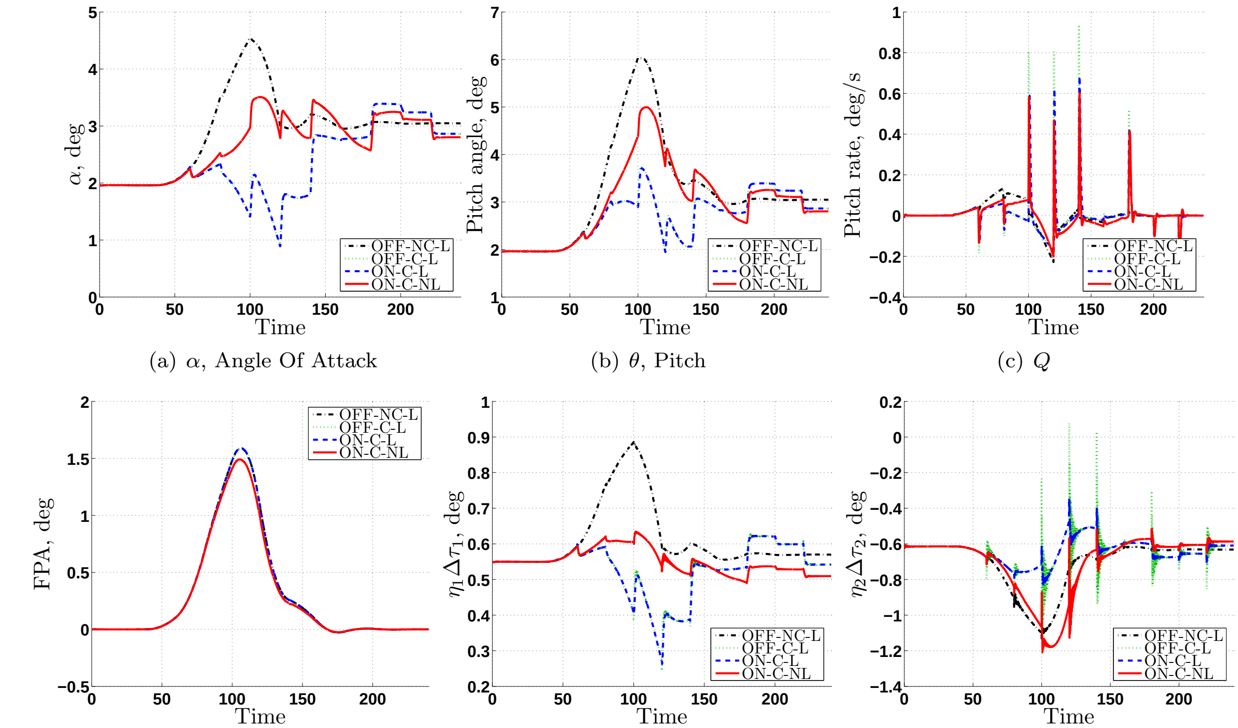

(a) α, Angle Of Attack (b) θ, Pitch (c) Q

(d) FPA, Flight Path Angle (e) $\eta_1\Delta\tau_1$ (f) $\eta_2\Delta\tau_2$

Figure 10. Selected states of the system.

References

[1]Thompson, E., Henry, K., and Williams, L., "Faster Than a Speeding Bullet: Guinness Recognizes NASA Scramjet," http://www.nasa.gov/home/hqnews/2005/jun/HQ_05_156_X43A_Guinness.html, June 2005.

[2]Bolender, M. A. and Doman, D. B., "A Non-Linear Model for the Longitudinal Dynamics of a Hypersonic Air-breathing Vehicle," Air Force Research Laboratory, Wright-Patterson AFB, OH 45433.

[3]Schmidt, D. K., "Integrated Control of Hypersonic Vehicles - A Necessity Not Just a Possibility," *AIAA Paper*, , No. AIAA-93-3761-CP, 1993, pp. 539–549.

[4]McRuer, D., "Design and Modeling Issues for Integrated Airframe/Propulsion Control of Hypersonic Flight Vehicles," American Control Conference, Boston, MA, 1992, pp. 729–734.

[5]Schmidt, D. K. and Chavez, F. R., "Analytical aeropropulsive/aeroelastic hypersonic-vehicle model with dynamic analysis," *Journal of Guidance, Control, and Dynamics*, Vol. 17, No. 6, 1994, pp. 1308–1319.

[6]Groves, K. P., Sigthorsson, D. O., Serrani, A., Yurkovich, S., Bolender, M. A., and Doman, D. B., "Reference Command Tracking for a Linearized Model of an Air-breathing Hypersonic Vehicle," *AIAA Guidance, Navigation, and Control Conference*, 2005.

[7]Marrison, C. I. and Stengel, R. F., "Design of robust control systems for a hypersonic Aircraft," *Journal of Guidance, Control, and Dynamics*, Vol. 21, No. 1, Jan.-Feb. 1998, pp. 58–63.

[8]Xu, H., Mirmirani, M. D., and Ioannou, P. A., "Adaptive Sliding Mode Control design for a hypersonic flight vehicle," *Journal of Guidance, Control, and Dynamics*, Vol. 27, No. 5, Sept.-Oct. 2004, pp. 829–838.

[9]Betts, J. T., "Survey of numerical methods for trajectory optimization," *Journal of Guidance, Control, and Dynamics*, Vol. 21, No. 2, March-April 1998, pp. 193–207.

[10]Bodson, M., "Evaluation of optimization methods for control allocation," *Journal of Guidance, Control, and Dynamics*, Vol. 25, No. 4, March-April 2002, pp. 703–711.

[11]Faiz, N. and Agrawal, S. K., "Trajectory planing of differentially flat systems with dynamics and inequalities," *Journal of Guidance, Control, and Dynamics*, Vol. 24, No. 2, March-April 2001, pp. 219–227.

[12]Harkegard, O. and Glad, S. T., "Resolving actuator redundancy - optimal control vs. control allocation," *Automatica*, Vol. 41, No. 1, Jan. 2005, pp. 137–144.

[13]Nieuwstadt, M. J. V. and Murray, R. M., "Real-time trajectory generation for differentially flat systems," *Int. J. Robust Nonlinear Control*, Vol. 8, No. 11, Sept. 1998, pp. 995–1020.

[14]Johansen, T. A. and Sbarbaro, D., "Lyapunov-based optimizing control of nonlinear blending processes," *IEEE Transactions on Control Systems Technology*, Vol. 13, 2005, pp. 631–638.

[15]Francis, B., "The linear multivariable regulator problem," *SIAM J. Contr. Optimiz.*, Vol. 15, 1977, pp. 486–505.

[16]Hautus, M., "Linear matrix equations with applications to the regulator problem," *Outils and Modeles Mathematique pour l'Automatique (I. D. Landau, ed.)*, Vol. 3, 1983, pp. 399–412.

[17]Isidori, A., Knobloch, H. W., and Flockerzi, D., *Topics in Control Theory*, Birkhaüser, 1993.

[18]Bay, J. S., *Fundamental of Linear State Space Systems*, McGraw-Hill, 1999.

[19]Nocedal, J. and Wright, S. J., *Numerical Optimization*, Springer Verlag, 1999.

[20]Groves, K. P. and Sigthorsson, D. O., "Hypersonic Air-breathing Model Implementation using Simulink," Department of Electrical Engineering The Ohio State University Columbus, OH 43210 USA.